

ARTICLE

Theoretical Study of Haloacetonitrile Anions: CH_2XCN^- ($\text{X}=\text{F}, \text{Cl}$)Xin-wen Zhang^a, Mei Li^b, Shan-xi Tian^{a,b*}

a. Hefei National Laboratory for Physical Sciences at Microscale, University of Science and Technology of China, Hefei 230026, China

b. Department of Chemical Physics, University of Science and Technology of China, Hefei 230026, China

(Dated: Received on August 28, 2007; Accepted on December 20, 2007)

Haloacetonitrile anions CH_2XCN^- ($\text{X}=\text{F}, \text{Cl}$) were studied by HF-SCF, Becke3-LYP, and MP2 methods together with the Dunning's basis set aug-cc-PVTZ. The vertical electron attachments to the neutral are endothermic. The geometrically optimized CH_2FCN^- is mainly a valence-bounded anion and $\text{CH}_2\text{FCN}^- \rightarrow \text{CH}_2\text{CN} + \text{F}^-$ is a nonadiabatic dissociation. This theoretical study in good agreement with the experimental results shows that the Becke3-LYP method is reasonable in describing the electronic structures of anions and dissociative attachment dynamics, while significant differences between MP2 and Becke3-LYP results are shown for the dissociation potential curves of $\text{CH}_2\text{ClCN}^- \rightarrow \text{CH}_2\text{CN} + \text{Cl}^-$.

Key words: Haloacetonitrile, Electron attachment, Dissociation dynamics, Electron correlation effect

I. INTRODUCTION

Anions of the molecules having large values of dipole moments (μ) attract great interest of both experimental and theoretical studies, because two typical anions, the dipole-bounded and the valence-bounded, may be involved in the processes and the various fragments produced after electron-attachment can be observed [1,2]. This resonance anionic state can be reached when the electron has low impact energy. A short-lived anion may dissociate, which is usually called a dissociative attachment [2]. Whether an anion is rather stable or unstable, some questions arise as to which type (the dipole-bounded or valence-bounded) anion might be formed; where they might be whereafter coupled or transferred, and which type of anion is correlated more strongly with the dissociation for the molecules with large μ value.

As a typical case, electron attachment to haloacetonitrile (CH_2XCN , $\text{X}=\text{F}, \text{Cl}, \text{Br}, \text{I}$) has been studied using the electron-beam [3,4] and the variable-temperature, flowing-after glow Langmuir-probe [5] techniques. In particular, Hacıoglu *et al.* found that five ionic products (F^- , CN^- , CFCN^- , CHCN^- , and CHFCN^-) were given off via a single dissociative attachment resonance at the electron energy of 0.8 eV for CH_2FCN , while only the Cl^- ionic product was dominated for CH_2ClCN at the low electron energy [3]. For comparison, the dominated ionic product CH_2CN^- appeared at 2.35 ± 0.1 eV for CH_3CN [6]. Competition between X^- and CN^- was investigated for the electron attachment to ClCN and BrCN , in which two different dissociation channels, ($\text{X} + \text{CN}^-$) or ($\text{X}^- + \text{CN}$), were proposed [7]. It is

well-known that the cyano group (CN) is treated as a pseudo halogen in inorganic chemistry, and it has a remarkable electron affinity (EA) value (3.82 eV) [8] which is a little larger than the halogens ($EA_{\text{F}}=3.40$ eV, $EA_{\text{Cl}}=3.62$ eV, $EA_{\text{Br}}=3.36$ eV) [9]. Although haloacetonitrile has a large μ value, there is an argument about which group the additional electron should be attached to. Namely, on the basis of the nature of the large EA values of cyano group and halogens, the additional electron could be attached to either of them. On the other hand, it is unclear that the low-energy electron can occupy the antibonding σ_{CX}^* or π_{CN}^* orbital in the valence-bounded anion. Unfortunately, until now there have been no *ab initio* level calculations on the molecular properties and the energy surfaces of the haloacetonitrile anions. A theoretical study on the molecular properties and dissociation dynamics of CH_2FCN^- and CH_2ClCN^- is reported in this work.

II. COMPUTATIONAL METHOD

It is noted that there are two different energies of electron attachment (EEA): vertical EEA (EEA_{v}) corresponding to the vertical attachment with the neutral molecular nucleic skeleton and adiabatic EEA (EEA_{a}) corresponding to the geometrically relaxed anion. An excess electron is assumed to be attached loosely in the former (the dipole-bounded) or to be bounded a little more tightly in the latter (valence-bounded anion). Therefore, using the neutral molecular equilibrium geometry (M), we can calculate

$$EEA_{\text{v}} = E_{\text{tot}}^{\text{a}}(M) - E_{\text{tot}}^{\text{n}}(M) \quad (1)$$

where $E_{\text{tot}}^{\text{a}}$ and $E_{\text{tot}}^{\text{n}}$ are the total energies of the anion and neutral one, respectively. EEA_{a} including zero-point vibrational energy (ZPVE) correction can be pre-

* Author to whom correspondence should be addressed. E-mail: sxtian@ustc.edu.cn

dicted as

$$\begin{aligned} EEA_a &= E_{\text{tot}+\text{ZPVE}}^a(A) - E_{\text{tot}+\text{ZPVE}}^n(M) \\ &= \Delta E_e + \Delta E_n \end{aligned} \quad (2)$$

where A in $E_{\text{tot}+\text{ZPVE}}^a(A)$ represents the anionic equilibrium geometry, and ΔE_e and ΔE_n are the electronic and nucleic contributions, respectively.

Similarly, the adiabatic dissociation energies (D_a) of anions can be calculated as the differences between the summarized energies of fragments (F_i , denoting the equilibrium structure) for a certain channel (j) and the total energy of an initial neutral molecule with ZPVE corrections

$$D_{aj} = \sum_i [E_{\text{tot}+\text{ZPVE}}(F_{ij})] - E_{\text{tot}+\text{ZPVE}}(M) \quad (3)$$

Considering the direct dissociation following the electron attachment, we can calculate the direct dissociation energies (D_d) using the geometrical parameters of the neutral molecules

$$D_{dj} = \sum_i [E_{\text{tot}}(F_{ij}^M)] - E_{\text{tot}}(M) \quad (4)$$

where F_{ij}^M denotes the particular moiety in the neutral geometry. The standard counterpoise (CP) technique [10] is used for correcting basis-set-superposition errors (BSSE) in the D_{dj} calculations,

$$D_{dj}^{CP} = \sum_i [E_{\text{tot}}^*(F_{ij}^M)] - E_{\text{tot}}(M) \quad (5)$$

where $E_{\text{tot}}^*(F_{ij}^M)$ is calculated using the molecular basis sets.

All calculations were performed using Gaussian 98 package [11]. The Hartree-Fock self-consistent field method (HF-SCF) and the Becke's three parameter hybrid functional method (Becke3-LYP) [12] with Dunning's correlation consistent triple-zeta basis set augmented with diffuse functions (aug-cc-pVTZ) [13] were used for the geometrical optimizations and energy calculations. The second-order Møller-Plesset perturbation method (MP2) [14] was used for comparison with the above two methods. Although the dispersion interactions are neglected in the density functional theory methods, Becke3-LYP has been successful (or equivalent to MP2) in predicting geometries, binding energies and frequencies for many hydrogen-bonding species in which the dispersion interactions are usually considered to be extremely important [15]. Moreover, the accuracy for predicting anionic properties at the Becke3-LYP level has been demonstrated elsewhere [16,17]. All optimized geometries were confirmed to be the minima on the respective energy surfaces by the analytical frequency calculations at the HF-SCF and Becke3-LYP levels. Spin contamination was checked in the

open-shell calculations. To elucidate the nature of electron attachments to CH_2FCN and CH_2ClCN , the natural charge analysis was made using the NBO 3.0 program [18] implemented in Gaussian 98. The present NBO analysis transformed the delocalized Becke3-LYP molecular orbital into localized orbital, providing insights into the chemical bonding characteristics in the neutral molecules and their anions.

III. RESULTS AND DISCUSSION

A. Electron attachment

The ground-state haloacetonitriles (CH_2FCN and CH_2ClCN), their anions, and the polyatomic fragments are shown in Fig.1 on the basis of the Becke3-LYP optimization calculations. The geometrical parameters and harmonic frequencies of the haloacetonitriles and their anions are given in Table I. For the neutral, the HF-SCF and Becke3-LYP calculations predicted the similar geometrical parameters, except for the small discrepancy ($\leq 0.036 \text{ \AA}$) of bond length; the harmonic vibrational frequency for each mode predicted at the Becke3-LYP level is distinctly smaller than that predicted at the HF-SCF level, indicating the different slopes of the molecular potential energy surfaces around the minima. For the anions, the discrepancies between the HF-SCF and Becke3-LYP results become more significant for CH_2FCN^- , and furthermore, the structure of anion CH_2ClCN^- predicted at the HF-SCF level distinctly differs from that at the Becke3-LYP level. The bond CCl in this anion is predicted to be dissociated by the Becke3-LYP calculation, however, there are no significant differences between the structures of

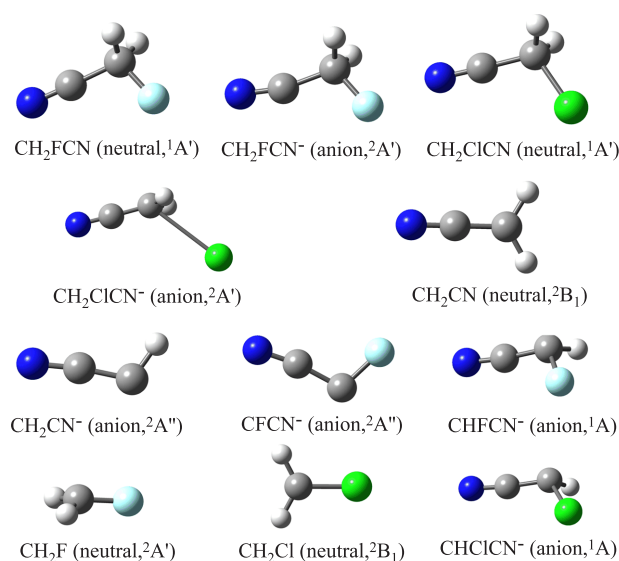


FIG. 1 Equilibrium geometrical configurations of CH_2XCN , CH_2XCN^- ($X=\text{F},\text{Cl}$), and polyatomic fragments.

TABLE I Geometrical parameters (R in Å and A in $^\circ$) and harmonic frequencies (cm^{-1}) of haloacetonitriles and anions

	Neutral			Anion		
	HF-SCF	Becke3-LYP	MP2	HF-SCF	Becke3-LYP	MP2
CH₂FCN						
$R(\text{CC})$	1.474	1.464	1.466	1.478	1.456	1.469
$R(\text{CH})$	1.080	1.091	1.088	1.080	1.098	1.092
$R(\text{CN})$	1.125	1.149	1.170	1.127	1.160	1.170
$R(\text{CF})$	1.348	1.384	1.380	1.353	1.403	1.385
$A(\text{CCN})$	178.3	178.6	178.6	179.3	166.1	178.6
$A(\text{CCF})$	110.3	110.6	110.1	109.1	111.8	109.3
$A(\text{HCF})$	109.2	108.6	108.8	109.7	107.4	109.3
	257.5(A')	225.3(A') ^a		255.3(A')	187.1(A') ^a	
	398.9(A'')	352.1(A'') ^b		395.9(A'')	296.1(A'') ^b	
	629.3(A')	572.4(A') ^c		633.2(A')	517.4(A') ^c	
	975.1(A')	925.4(A') ^d		955.6(A')	888.3(A') ^d	
	1136.8(A'')	1032.5(A'') ^e		1110.4(A'')	943.6(A') ^f	
	1214.1(A')	1061.2(A') ^f		1184.6(A')	988.6(A'') ^e	
	1388.0(A'')	1264.3(A'') ^g		1381.6(A'')	1208.4(A'') ^g	
	1540.7(A')	1399.6(A') ^h		1537.4(A')	1328.6(A') ^h	
	1623.2(A')	1486.5(A') ⁱ		1611.9(A')	1431.3(A') ⁱ	
	2600.8(A')	2365.2(A') ^j		2587.9(A')	2173.6(A') ^j	
	3230.4(A')	3055.8(A') ^k		3219.2(A')	2944.6(A') ^k	
	3279.7(A'')	3098.7(A'') ^l		3273.2(A'')	2968.4(A'') ^l	
CH₂ClCN						
$R(\text{CC})$	1.463	1.452	1.456	1.465	1.380	1.458
$R(\text{CH})$	1.076	1.086	1.086	1.077	1.076	1.091
$R(\text{CN})$	1.126	1.149	1.171	1.126	1.168	1.171
$R(\text{CCl})$	1.779	1.805	1.781	1.790	2.973	1.794
$A(\text{CCN})$	178.4	178.7	178.8	179.9	178.8	179.4
$A(\text{CCCl})$	111.4	111.6	110.9	109.9	127.1	109.7
$A(\text{HCCl})$	108.0	107.5	108.0	108.4	87.17	108.1
	209.2(A')	188.0(A') ^a		209.4(A')	39.85(A') ^m	
	403.7(A'')	359.6(A'') ^b		401.4(A'')	168.8(A'') ^f	
	544.6(A')	490.0(A') ^c		541.4(A')	171.3(A'') ^g	
	816.0(A')	728.7(A') ^d		787.4(A')	406.3(A'') ^b	
	1001.5(A'')	919.9(A'') ^e		982.9(A'')	483.3(A') ^c	
	1009.3(A')	951.1(A') ^f		983.6(A')	602.8(A') ^h	
	1314.3(A'')	1201.7(A'') ^g		1302.1(A'')	1015.8(A'') ^e	
	1420.1(A')	1287.6(A') ^h		1418.3(A')	1057.9(A') ^f	
	1595.4(A')	1467.6(A') ⁱ		1576.0(A')	1423.8(A') ⁱ	
	2600.1(A')	2360.4(A') ^j		2589.3(A')	2143.5(A') ^j	
	3257.1(A')	3090.7(A') ^k		3233.1(A')	3198.2(A') ^k	
	3315.9(A'')	3141.6(A'') ^l		3291.0(A'')	3293.8(A'') ^l	

^a N in-plane wagging.^b CCN out-of-plane bending.^c CCN in-plane bending.^d CCF(Cl) bending.^e CH₂ out-of-plane wagging.^f CC, CF(Cl) stretching.^g CH₂ asymmetric wagging.^h CH₂ symmetric wagging.ⁱ HCH bending.^j CN stretching.^k CH symmetric stretching.^l CH asymmetric stretching.^m Cl in-plane wagging.

TABLE II Natural charge analysis, electronic spatial extension ($\langle R \rangle^2$ in a.u.), and dipole moments (μ in Debye) of haloacetonitriles and anions^a

		Neutral	Vertical-Attached anion	Adiabatic anion
CH ₂ FCN	C(H)	-0.01164	-0.10915	-0.12453
	H	0.20349	-0.20474	-0.15858
	C	0.22877	0.25157	0.22275
	F	-0.34948	-0.36870	-0.38386
	N	-0.27463	-0.36424	-0.39721
	$\langle R \rangle^2$	270.2(265.6)	338.3(343.1)	337.1(342.6)
	μ	3.26(3.51)	5.57(7.84)	4.22(7.93)
CH ₂ ClCN	C(H)	-0.44160	-0.57622	-0.42143
	H	0.24669	-0.06076	0.22557
	C	0.25033	0.27092	0.20620
	Cl	-0.02509	-0.20528	-0.82974
	N	-0.27702	-0.36790	-0.40617
	$\langle R \rangle^2$	401.3(396.2)	463.9(474.3)	698.5(471.7)
	μ	3.28(3.49)	6.95(9.22)	3.89(9.33)

^a The data were calculated at the Becke3-LYP level; the values of $\langle R \rangle^2$ and μ in parenthesis were predicted at the HF-SCF level.

the neutral and the anionic CH₂ClCN by the HF-SCF calculations. It is interesting to compare the structural parameters and vibrational frequencies of the neutral with those of the anion predicted at the Becke3-LYP level. The bond lengths $R(\text{CX}, \text{X}=\text{F}, \text{Cl})$ and $R(\text{CN})$ are elongated and the bond angles $A(\text{CCX})$ are widened from the neutral to the anions. The sequence for two vibrational modes ($1032.5 \text{ cm}^{-1}\text{A}''$, CH₂ out-of-plane wagging and $1061.2 \text{ cm}^{-1}\text{A}'$, CC, CF stretching) is reversed ($943.6 \text{ cm}^{-1}\text{A}'$ and $988.6 \text{ cm}^{-1}\text{A}''$), from CH₂FCN to CH₂FCN⁻. Due to the dissociation between Cl⁻ and CH₂CN in the anion, the lowest frequency $39.85 \text{ cm}^{-1}\text{A}'$ is noted as Cl in-plane wagging; the other two low frequencies $168.8 \text{ cm}^{-1}\text{A}''$ and $171.3 \text{ cm}^{-1}\text{A}''$ correspond to CCl stretching and CH₂ wagging. This low value of the CH₂ wagging frequency may be explained by the weak interactions between Cl⁻ and CH₂CN (see Fig.1). The frequencies $406.3 \text{ cm}^{-1}\text{A}''$, $483.3 \text{ cm}^{-1}\text{A}'$, $602.8 \text{ cm}^{-1}\text{A}'$, $1015.8 \text{ cm}^{-1}\text{A}''$, and $1057 \text{ cm}^{-1}\text{A}'$ of CH₂ClCN⁻ are close to those of the radical CH₂CN ($386.9 \text{ cm}^{-1}\text{B}_2$, $434.2 \text{ cm}^{-1}\text{B}_1$, $680.7 \text{ cm}^{-1}\text{B}_1$, $1036.5 \text{ cm}^{-1}\text{B}_2$, and $1058.0 \text{ cm}^{-1}\text{A}_1$). It is also interesting to compare the HF-SCF and Becke3-LYP with the MP2 results. For the neutral, the results given by the MP2 calculations are a little closer to those predicted by the Becke3-LYP; while the MP2 results are closer to the HF-SCF for the anions, in particular, for CH₂ClCN⁻. In general the distinct discrepancy of the anionic structures between CH₂FCN⁻ and CH₂ClCN⁻ predicted at the Becke3-LYP level indicates that the dissociation dynamics should be different.

In Table II, the natural charge analysis and the other electronic properties of the anions are presented to-

gether with the properties of the neutral for comparison. For the neutral, the Becke3-LYP calculations predict that the haloacetonitriles will have similar μ values vectoring from the halogen and cyano (negative) to CH₂ group (positive). One may notice that the negative charge of F is much larger than the Cl charge, presumably interpreted by the different intramolecular interactions between the halogen and cyano group [19]. When an electron is vertically attached to CH₂FCN, the CH₂ group is charged negatively (totally ~ -0.914) and only a little negative charge is added to F and N atoms that are negatively charged with almost equivalent populations, which is different from the neutral and the adiabatic anion. With the geometrical relaxation due to the electron-nuclei correlations, the negative charge on the CH₂ group transfers to F and N atoms in the adiabatic anion. The similar situation occurs in CH₂ClCN⁻. Although the very small negative charge is still localized on the CH₂ group, the larger negative charge transfers to Cl; finally the Cl atom charged with a negative unit is dissociated for the adiabatic CH₂ClCN⁻ anion. On the basis of the above natural charge analysis at the Becke3-LYP level, the conclusions can be derived: these vertical-attached anions can be of the dipole-bounded type; the relaxed adiabatic anion CH₂FCN⁻ is still partly dipole-bounded but mainly valence-bounded π_{CN}^* (negative charge increases ~ -0.13 on the bond CN with respect to that in the neutral); the adiabatic anion CH₂ClCN⁻ can be treated as hydrogen-bonding and electrostatic bounded ($\text{Cl}^{-0.82974} \dots \text{H}^{2 \times (+0.22557)}$) cluster. Moreover, the electronic spatial extension $\langle R \rangle^2$ and dipole moment also indicate that the additional electron should be bounded in the different types, because the vertical-attached an-

TABLE III Energies of vertical electron attachment (EEA_v), adiabatic energies of electron attachment (EEA_a) and their electronic (ΔE_e) and nucleic (ΔE_n) contributions, All values are in kJ/mol

		EEA_v	EEA_a	ΔE_e	ΔE_n
CH ₂ FCN	HF-SCF	56.0861	54.9326	55.6991	-0.7665
	Becke3-LYP	21.4250	12.5001	18.2606	-5.7605
	MP2	42.9655		42.7216	
CH ₂ ClCN	HF-SCF	55.6907	54.1422	55.1660	-1.0238
	Becke3-LYP	16.9268	-151.8056	-138.7569	-13.0486
	MP2	38.3376		37.9188	

ions have much larger values respective to the adiabatic anions. The extremely large $\langle R \rangle^2$ value of the adiabatic CH₂ClCN⁻ anion is due to the Cl dissociation predicted at the Becke3-LYP level. The HF-SCF calculations predict the very large values of the $\langle R \rangle^2$ (except for the $\langle R \rangle^2$ of the adiabatic CH₂ClCN⁻ anion) and the exaggeratedly large μ values of the anions, indicating that the electron correlation is necessary to be precisely describe the electronic structures of anions.

Accordingly, the electron densities of the lowest unoccupied molecular orbitals (LUMOs) and the single occupied molecular orbital (SOMOs) of vertical-attached and adiabatic anions have been plotted in Fig.2. The HF-SCF calculations predicted the diffuse electron distributions of LUMOs of CH₂FCN and CH₂ClCN and the additional electron is occupied at this diffuse orbital or is bounded diffusely, the electron distributions predicted at the Becke3-LYP level are distinctly different between the neutral LUMO and the anionic SOMO. Although the vertically-attached electron may be bounded diffusely around the CH₂ group, the electron distribution mainly appears as the antibond π_{CN}^* in the SOMO of CH₂FCN (see Fig.2(a)) and as the antibond σ_{CCl}^* (actually the Cl3p in-plane orbital) in the SOMO of CH₂ClCN⁻ (see Fig.2(b)). All differences for the anions predicted at the HF-SCF and Becke3-LYP levels may be explained by the following facts: the long-range Coulomb interactions in the HF scheme lead to the diffuse electron distributions, while the short-ranged dipole interactions can be treated well with electron correlations in the Becke3-LYP functional.

The values of EEA_v and EEA_a defined by Eq.(1) and Eq.(2) were calculated and are summarized in Table III. It is surprising that the HF-SCF level of theory predicted the similar EEA values between CH₂FCN and CH₂ClCN, and these values are much larger than the Becke3-LYP results. To our surprise, the MP2 data are quite close to the HF-SCF ones. The positive attachment energies of the vertical attachment to CH₂FCN and CH₂ClCN and the positive adiabatic attachment energy of CH₂FCN imply that it is endothermic, which is in line with the experimental results [5]. The negative EEA_a predicted by the Becke3-LYP calculations supports the experimental conclusion of the exothermic reaction to produce the Cl⁻ [5], but both the positive

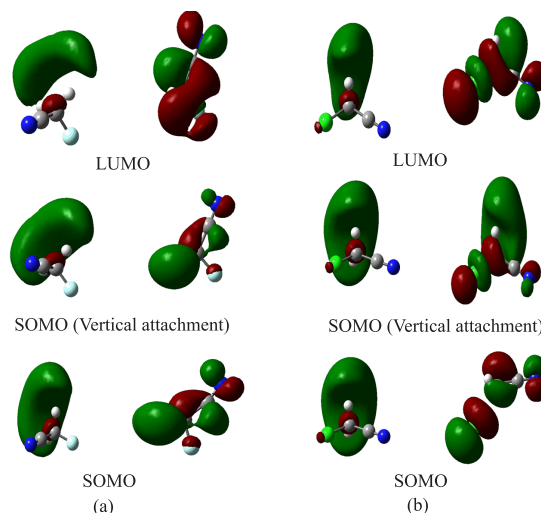


FIG. 2 Electron populations of molecular orbital of CH₂FCN (LUMO), the vertical attached anion CH₂FCN⁻ (SOMO), and the adiabatic anion CH₂FCN⁻ (SOMO) in (a) and CH₂ClCN (LUMO), the vertical attached anion CH₂ClCN⁻ (SOMO), and the adiabatic anion CH₂ClCN⁻ (SOMO) in (b) calculated at the HF-SCF (left) and Becke3-LYP (right) levels.

EEA_v and ΔE_e given by the MP2 calculations imply the contrary conclusion. Furthermore, the nucleic contributions ΔE_n to EEA_a indicate that the geometrical relaxation owing to the electron attachment is predicted to be significant at the Becke3-LYP level. The theoretical comparison suggests that the second-order perturbation corrections to the HF wave functions in the MP2 scheme may be inadequate for these anions, and the short-ranged interactions between an attached electron and the target molecule can be reasonably described by the hybrid exchange-correlation functional. According to the anionic stability respective to the neutral [2], the present Becke3-LYP calculations predict that the CH₂FCN⁻ is at the shape-resonance state while CH₂ClCN⁻ is at the Feshbach-resonance state.

B. Dissociation dynamics

Five fragments (CHCN⁻, F⁻, CN⁻, CFCN⁻, and CHF₂CN⁻) were observed at the collision energy of

0.8 eV, with an intensity ratio 1000:250:4:3:3 [3]. The calculated D_a and D_d energies of the above dissociated processes as well as those for CH_2ClCN^- are listed in Table IV. The BSSE corrections to D_d are very small (<9.36 kJ/mol) because the large basis set aug-cc-PVTZ was used throughout the calculations. The D_a values were predicted to be much smaller than the D_d values for CH_2FCN^- , which is contrast to the dissociation processes of Cl^- , CN^- , and H from CH_2ClCN^- at the Becke3-LYP level of theory. The energies D_d for two atoms dissociated from the parent anion are more than 418 kJ/mol, due to two bonds being broken. The recombination of two dissociated atoms reduces the dissociation energies significantly (see the D_a values in Table IV). Unfortunately, the strong spin contaminant ($\langle S^2 \rangle > 0.8$) was found in the

TABLE IV Adiabatic dissociation energies (D_a in kJ/mol) with zero-point-vibration energy (ZPVE) corrections and directed dissociation energies with the standard counterpoise for basis-set-superposition-error corrections (D_d^{CP} in kJ/mol).

	HF-SCF	Becke3-LYP
$\text{CH}_2\text{FCN}^- \rightarrow \text{CHCN} + \text{HF}^a$		
D_d	49.54	42.01
D_d^{CP}	777.35	629.32
$\text{CH}_2\text{FCN}^- \rightarrow \text{CH}_2\text{CN} + \text{F}$		
D_d	45.56	33.26
D_d^{CP}	118.66	178.41
$\text{CH}_2\text{FCN}^- \rightarrow \text{CH}_2\text{F} + \text{CN}^-$		
D_a	37.45	67.70
D_d^{CP}	84.56	106.98
$\text{CH}_2\text{FCN}^- \rightarrow \text{CFCN}^- + \text{H}_2^a$		
D_d	125.35	105.48
D_d^{CP}	641.07	556.01
$\text{CH}_2\text{FCN}^- \rightarrow \text{CHFCN}^- + \text{H}$		
D_d	204.14	195.94
D_d^{CP}	258.82	240.20
$\text{CH}_2\text{ClCN}^- \rightarrow \text{CH}_2\text{CN} + \text{Cl}^-$		
D_d	-144.85	56.99
D_d^{CP}	-80.08	-50.79
$\text{CH}_2\text{ClCN}^- \rightarrow \text{CH}_2\text{Cl} + \text{CN}^-$		
D_d	24.85	220.62
D_d^{CP}	82.22	109.96
$\text{CH}_2\text{ClCN}^- \rightarrow \text{CHCN}^- + \text{HCl}^a$		
D_d	52.05	217.74
D_d^{CP}	570.66	487.14
$\text{CH}_2\text{ClCN}^- \rightarrow \text{CHClCN}^- + \text{H}$		
D_d	154.93	322.46
D_d^{CP}	202.34	200.29

^a For the calculations of D_d^{CP} values, HF, HCl, and H_2 are treated as two fragments rather than molecules.

MP2 calculations for the adiabatic and direct dissociations to produce F^- or Cl^- . The HF-SCF calculations indicate that these dissociation processes except for $\text{CH}_2\text{ClCN}^- \rightarrow \text{CH}_2\text{CN} + \text{Cl}^-$ are endothermic, which is consistent with the Becke3-LYP results. The D_a values suggest that the processes $\text{CH}_2\text{FCN}^- \rightarrow \text{CH}_2\text{CN} + \text{F}^-$ and $\text{CH}_2\text{FCN}^- \rightarrow \text{CHCN}^- + \text{HF}$ are energetically favorable with respect to the others. The observation of the higher intensity of CHCN^- with respect to that of F^- [3] perhaps suggests that the anion F^- reacts with the CH_2CN radical to produce more CHCN^- . The energetic sequence of the D_a to produce CN^- , CFCN^- , and CHFCN^- , given by the Becke3-LYP calculations, are in good agreement with the observations [3]. Moreover, the D_a energies to produce CN^- , CHCN^- , and CHClCN^- are much larger than those to produce Cl^- for CH_2ClCN^- at the Becke3-LYP level. In particular, the negative D_d value (-50.75 kJ/mol) for the Cl^- fragment indicates that the process $\text{CH}_2\text{ClCN}^- \rightarrow \text{CH}_2\text{CN} + \text{Cl}^-$ may be a direct (fast) dissociation while $\text{CH}_2\text{FCN}^- \rightarrow \text{CH}_2\text{CN} + \text{F}^-$ undergoes a temporary stable anionic state, at the Becke3-LYP theoretical level. Moreover, on the basis of the experimental spectra (Fig.2 in Ref.[3]), one can estimate that the appearance energy (electron energy at the half height of the integrated spectra) is about 0.4 eV for the fragments F^- , CN^- , and CHCN^- while it this value is a little larger for CFCN^- and CHFCN^- . The Becke3-LYP calculations give the D_a values: 0.345 eV (F^-), 0.435 eV (CHCN^-), 0.70 eV (CN^-), 1.093 eV (CFCN^-), and 2.03 eV (CHFCN^-). The appearance energy of Cl^- may be negative from Fig.1 in Ref.[3], supported by the D_d value (-50.75 kJ/mol, ~ -0.526 eV) in this work. In Fig.1 and Fig.2 of Ref.[3], the band shape of Cl^- differs significantly from that of F^- besides the peak positions: the former has a big tail extending to the high electron energy while the latter is a symmetric peak. This suggests that the potential energy curve for $\text{CH}_2\text{ClCN}^- \rightarrow \text{CH}_2\text{CN} + \text{Cl}^-$ is decreasingly sharper than that of $\text{CH}_2\text{FCN}^- \rightarrow \text{CH}_2\text{CN} + \text{F}^-$, on the basis of the reflection principle of the potential energy curves [2,20,21]. This will be proved by the further calculations given below.

The relaxed potential energy curves are plotted in Fig.3 with the Becke3-LYP calculations by scanning bond lengths CC and CF or CCl of the neutral and anions. One can find the distinct differences between these two molecules: the dissociation energies of the CC bonds in the neutral CH_2FCN , CH_2ClCN , and anion CH_2ClCN^- are predicted to be extremely high, while it may be lower than 125.4 kJ/mol for CH_2FCN^- (Fig.3 (a) and (b)), the CF or CCl dissociation in anion becomes more energetically favorable than in the neutral, a temporary stable anionic state CH_2FCN^- exists, showing a local minimum point with an energy barrier about 6.7 kJ/mol, and a direct dissociation process is predicted along the CCl bond in CH_2ClCN^- , which is contrast to the increasing energies predicted

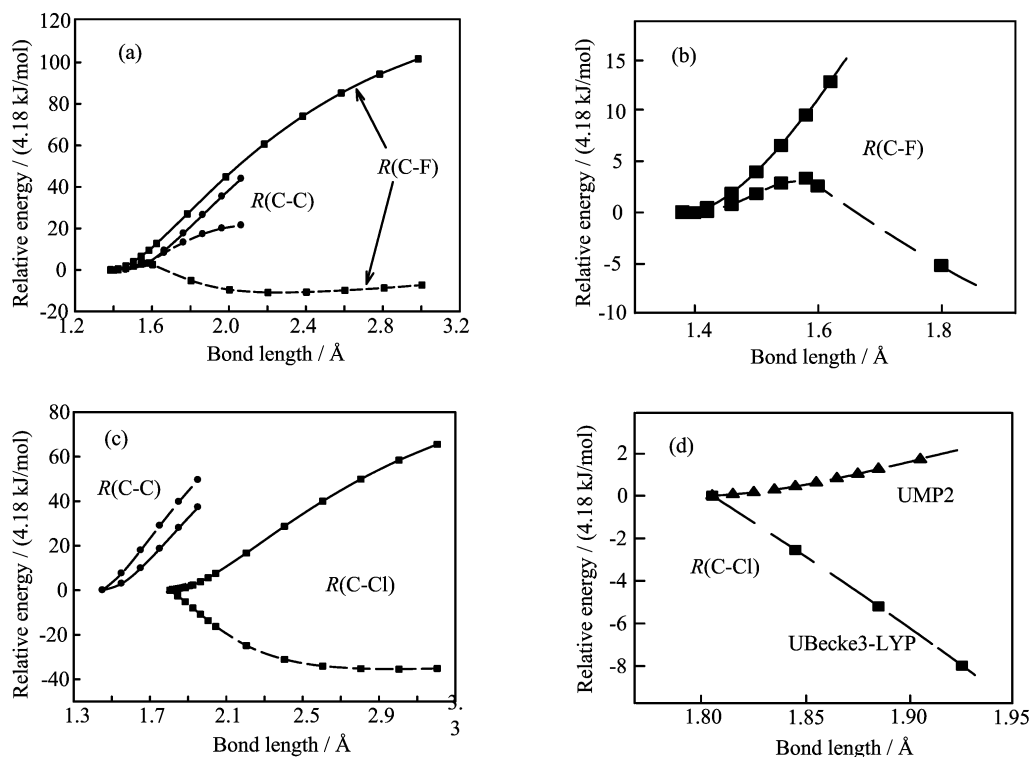


FIG. 3 Potential energy curves calculated by the relaxed scan at the Becke3-LYP level for dissociations CX bonds (X=F,Cl) in the neutral (solid line) and the anions (broken line), for dissociations CC bonds in the neutral (solid line) and anions (broken line); the energies are calibrated by the start point. CH₂FCN and CH₂FCN⁻ in (a) and (b), CH₂ClCN and CH₂ClCN⁻ in (c) and (d).

by the MP2 calculations (Fig.3 (c) and (d)). However, the above analyses on the experimental spectra support the Becke3-LYP results. In Fig.3(a), another minimum point exists at about 2.2 Å on the CF curve, about 60 meV lower than the transition state and less than 10 meV lower than the separated fragments. The latter smaller energy is mostly due to electrostatic interactions between F^{-δ1}...H^{2×(+δ2)}, which is similar to Cl^{-0.82974}...H^{2×(+0.22557)} in the anionic CH₂ClCN⁻.

IV. CONCLUSION

The molecular properties and dissociation dynamics were theoretically investigated together with analysis of the experimental spectra reported in Ref.[3]. Several different characteristics between CH₂FCN⁻ and CH₂ClCN⁻ are predicted by the Becke3-LYP calculations: (i) The additional electron is bounded diffusely (or dipole-bounded) in the vertical attachment, while the dipole-bounded electron may transfer to be valence-bounded (i.e. occupying π_{CN}^{*} for CH₂FCN⁻ or σ_{CCl}^{*} for CH₂ClCN⁻), finally to form Cl⁻ by occupying the Cl3p in-plane orbital. (ii) The vertical electron attachments to CH₂FCN and CH₂ClCN are endothermic and the geometrical relaxations of CH₂ClCN⁻ lead to the exothermic dissociation CH₂ClCN⁻→CH₂CN+Cl⁻. (iii) Calculations of dissociation energies can qualitatively in-

terpret the experimental spectra [3]. (iv) Further calculations of the potential energies indicate that CH₂FCN⁻→CH₂CN+F⁻ undergoes a temporary state and it is a nonadiabatic process, while CH₂ClCN⁻→CH₂CN+Cl⁻ is a typical direct dissociation process. Moreover, the HF-SCF calculations cannot give reasonable predictions for these two anions, and the distinctly different results for CH₂ClCN⁻ are predicted at the Becke3-LYP and MP2 levels of theory.

V. ACKNOWLEDGMENT

This work was supported by the Program of New-Century Excellent Talents in Universities, Ministry of Education of China.

- [1] C. Desfrancois, H. A. Carime, and J. P. Schermann, *Int. J. Mod. Phys. B* **10**, 1339 (1996).
- [2] E. Illenberger and J. Momigny, *Gaseous Molecular Ions, Topics in Physical Chemistry*, Vol. 2, H. Baumgürtel, E. U. Franck, and W. Grnbein, Eds., New York: Springer-Verlag, (1992).
- [3] J. Hacıoglu, S. Suzer, T. Oster, and E. Illenberger, *Chem. Phys. Lett.* **153**, 268 (1988).

- [4] M. Heni and E. Illenberger, *Int. J. Mass Spectrom. Ion Proc.* **73**, 127 (1986).
- [5] J. M. Van Doren, W. M. Foley, J. E. McClellan, T. M. Miller, A. D. Kowalak, and A. A. Viggiano, *Int. J. Mass Spectrom. Ion Proc.* **149-150**, 423 (1995).
- [6] W. Sailer, A. Pelc, P. Limão-Vieira, N. J. Mason, J. Limtrakul, P. Scheier, M. Probst, and T. D. M'ark, *Chem. Phys. Lett.* **381**, 216 (2003), and the references therein.
- [7] F. Bruning, I. Hahndorf, A. Stamatovic, and E. Illenberger, *J. Phys. Chem.* **100**, 19740 (1996).
- [8] R. Klein, R. P. McGinnis, and S. R. Leone, *Chem. Phys. Lett.* **100**, 475 (1983).
- [9] R. G. Pearson, *Inorg. Chem.* **27**, 734 (1988).
- [10] S. F. Boys and F. Bernardi, *Mol. Phys.* **19**, 553 (1970).
- [11] M. J. Frisch, G. W Trucks, H. B. Schlegel, G. E. Scuseria, M. A. Robb, J. R. Cheeseman, V. G. Zakrzewski, J. A. Montgomery, R. E. Stratmann, J. C. Burant, S. Dapprich, J. M. Millam, A. D. Daniels, K. N. Kudin, M. C. Strain, O. Farkas, J. Tomasi, V. Barone, M. Cossi, R. Cammi, B. Mennucci, C. Pomelli, C. Adamo, S. Clifford, J. Ochterski, G. A. Petersson, P. Y. Ayala, Q. Cui, K. Morokuma, D. K. Malick, A. D. Rabuck, K. Raghavachari, J. B. Foresman, J. Cioslowski, J. V. Ortiz, B. B. Stefanov, G. Liu, A. Liashenko, P. Piskorz, I. Komaromi, R. Gomperts, R. L. Martin, D. J. Fox, T. Keith, M. A. Al-Laham, C. Y. Peng, A. Nanayakkara, C. Gonzalez, M. Challacombe, P. M. W. Gill, B. G. Johnson, W. Chen, M. W. Wong, J. L. Andres, M. Head-Gordon, E. S. Replogle, and J. A. Pople, *Gaussian 98, Revision A.7*. Pittsburgh, PA: Gaussian, Inc., (1998).
- [12] (a) A. D. Becke, *J. Chem. Phys.* **98**, 5648 (1993).
(b) C. T. Lee, W. Yang, and R. G. Parr, *Phys. Rev. B* **37**, 785 (1988).
- [13] D. E. Woon and T. H. Jr. Dunning, *J. Chem. Phys.* **98**, 1358 (1993).
- [14] C. Møller and M. S. Plesset, *Phys. Rev.* **46**, 618 (1934).
- [15] L. Lundell and Z. Latajka, *J. Phys. Chem. A* **101**, 5004 (1997).
- [16] J. C. Rienstra-Kiracofe, G. S. Tschumper, and H. F. Schaefer III, *Chem. Rev.* **102**, 231 (2002).
- [17] N. I. Hammer, R. N. Compton, *Phys. Rev. Lett.* **92**, 083003 (2004).
- [18] E. D. Glendening, J. K. Badenhoop, A. E. Reed, J. E. Carpenter, and F. F. Weinhold, *Theoretical Chemistry Institute, NBO 3.0*, University of Wisconsin, Madsion, WI, (1996).
- [19] S. X. Tian, N. Kishimoto, and K. Ohno, *K. J. Phys. Chem. A* **107**, 485 (2003).
- [20] H. S. Taylor, in *Advances in Chemical Physics*, Vol. XVIII, S. A. Rice, Ed., New York: Interscience Publishers, (1970).
- [21] T. F. O'Malley, *Phys. Rev.* **150**, 14 (1966).